Well-width dependence of the optical anisotropies in (001) and (110) semiconductor quantum wells: The effect of spin-orbit split-off bands

Yasutomo Kajikawa*
Optoelectronics Technology Research Laboratory, 5-5 Tohkodai, Tsukuba, Ibaraki 300-26, Japan
(Received 28 November 1994; revised manuscript received 3 February 1995)

We have investigated both theoretically and experimentally the well-width dependence of the polarization anisotropies of the interband transitions in semiconductor quantum wells (QW's). In our theoretical study, we adopted the six-band Luttinger-Kohn model in which the spin-orbit split-off (SO) bands are included. The polarization-dependent optical-matrix elements at the Brillouin-zone center in (001) and (110) QW's were calculated as a function of the well width using the exact solutions of coupled effective-mass equations. The calculated results are shown for $GaAs/Al_xGa_{1-x}As$ and $Ga_{0.5}In_{0.5}P/(Al_xGa_{1-x})_{0.5}In_{0.5}P$ (001)-oriented QW's as well as $GaAs/Al_xGa_{1-x}As$ (110)-oriented QW's. In the (001) QW's, the inclusion of the SO bands into the calculation led to a decrease in the TM/TE ratio of the optical-matrix element for the light-hole transition with decreasing well width. In the $Ga_{0.5}In_{0.5}P/(Al_xGa_{1-x})_{0.5}In_{0.5}P$ system, which has a smaller spin-orbit splitting energy, the decrease in the TM/TE ratio was shown to be more remarkable to show reversal between the TM and TE strength when the hole confinement energy is large. In the (110) QW's, the effect of coupling to the SO bands was revealed to appear not only for the light-hole transition but also for the heavy-hole transition. The calculated results for (110) $GaAs/Al_xGa_{1-x}As$ QW's illustrated that the anisotropy regarding the polarization direction in the (110) QW plane increases with decreasing well width according to the increase in coupling to the SO bands. In order to investigate experimentally the well-width dependence of the in-plane optical anisotropy in (110) QW's, polarized photoluminescence measurements were performed at 77 K on (110) $GaAs/Al_{0.2}Ga_{0.8}As$ QW structures having various well widths. The in-plane anisotropy of heavy-hole excitonic emission was observed to be almost unchanged for well widths wider than 9 nm, while it was observed to increase for narrower well widths with decreasing well width. The degree of linear polarization observed in the photoluminescence measurements showed good agreement with the calculated results.

I. INTRODUCTION

One of the most distinctive features of semiconductor quantum wells (QW's), when compared with bulk semiconductors, is in their polarization properties. Whereas bulk III-V semiconductors with the zinc-blende-type structure are optically isotropic, QW's exhibit anisotropic polarization properties. This polarization anisotropy affects the characteristics of QW lasers.[1] Early in the development of QW lasers, it had already been noticed that QW lasers show different gain characteristics between TE and TM modes.[2,3] Yamanishi and Suemune[4] revealed that this difference between TE and TM is owing to the anisotropy in the optical-matrix elements in QW's. They showed that the optical-matrix element for the heavy-hole transition at the Brillouin-zone center has only the TE-mode component without the TM-mode component. It was also shown that the squared optical-matrix element for the light-hole transition is larger for TM than for TE by a factor of 4. These results are irrelevant to what materials the QW structure is composed of. The above-mentioned results were obtained within an effective-mass approximation based on the four-band model.[5]

In the four-band approximation, only the heavy- and light-hole bands are taken into account, while the spin-orbit split-off (SO) bands are neglected. This four-band model has been proved to be a fairly good approximation for $GaAs/Al_xGa_{1-x}As$ QW's, which have been most intensively investigated among various QW's. Not only the optical-matrix elements but also the energy levels have been calculated within this model in many studies on $GaAs/Al_xGa_{1-x}As$ QW's. The four-band approximation is considered to be justifiable in the case of $GaAs/Al_xGa_{1-x}As$ QW's because of the large spin-orbit splitting energy Δ in GaAs ($\sim$340 meV) compared with the quantum-confinement energies of holes.

Recently, however, studies on semiconductor QW's have spread from $GaAs/Al_xGa_{1-x}As$ QW's to a variety of QW's consisting of various materials including strained layers. Also, in theoretical treatments of the energy levels and optical properties of such QW's, the four-band approximation has often been used, as in the case of (001) $GaAs/Al_xGa_{1-x}As$ QW's, due to its simplicity.

Strictly speaking, however, the effect of SO bands should be incorporated into the rigorous calculations of the valence-subband structures, as has been pointed out by Schuurmans and co-workers.[6,7] Recently, it has been pointed out that the effect of the SO bands becomes significant in strained QW's, such as $In_xGa_{1-x}As/AlAs$ QW's (Ref. 8) and $In_xGa_{1-x}As/InP$ QW's,[9] especially when highly strained.

In addition to the above QW's, whose well layers comprise arsenide compound semiconductors, $Ga_{0.5}In_{0.5}P$ QW's have recently attracted much attention as the active region for a laser diode operating in the 600-nm range.[10] Since phosphide compound semiconductors generally have smaller spin-orbit splittings than do those of arsenide (see Table I in Sec. III), the effect of the SO bands is expected to be significant in $Ga_{0.5}In_{0.5}P$ QW's. (Generally, the spin-orbit splitting energy in the III-V compound semiconductor is dominated by the V element and is larger for a V element with a larger atomic number.[11]) A few authors[12–15] have recognized this point, and have thus calculated the energy levels in $Ga_{0.5}In_{0.5}P/(Al_xGa_{1-x})_{0.5}In_{0.5}P$ QW's in the six-band model instead of the conventional four-band model. In these studies, it has been revealed that the coupling of the SO bands affects the energy levels of light-hole subbands even at the zone center. On the other hand, however, there has been no calculation of the optical-matrix elements in this system using the six-band model, though it has already been pointed out by Eppenga, Schuurmans, and Colak[7] that the coupling of the SO bands also affects the optical-matrix elements. It is thus expected that the TM/TE ratio of the transition strength may be calculated to be different from the conventional value when the effect of the SO bands is taken into account.

Besides the anisotropy between TM and TE, there exists an additional optical anisotropy in differently oriented QW's than (001) and (111): optical anisotropy with respect to the rotation of the polarization vector in the plane of the QW. Such in-plane optical anisotropy in QW's grown on low-symmetry crystallographic planes was reported first for (110) $GaAs/Al_xGa_{1-x}As$ QW's.[16,17] After these reports, in-plane optical anisotropy has also been reported for (113) $GaAs/Al_xGa_{1-x}As$ QW's,[18] (110) $In_xGa_{1-x}As_yP_{1-y}$ QW's,[19] and (110) and (112) strained $In_xGa_{1-x}As/GaAs$ QW's.[20,21] These in-plane anisotropies in low-symmetry QW's have been proposed to be used for controlling and stabilizing the lasing mode of vertical-cavity surface-emitting lasers.[22–24]

In our previous studies[16,18] of (110) and (113) QW's, we investigated the in-plane optical anisotropy of rather wide QW's having well widths of 9–10 nm. In these studies as well as in other papers,[19,21] the in-plane optical anisotropy was analyzed within a four-band effective-mass model using the 4×4 Luttinger-Kohn Hamiltonian, while neglecting the SO bands. The four-band model offers simple analytical expressions for the in-plane optical anisotropies, whose expressions depend on material parameters (Luttinger parameters) but include neither the well width nor the barrier height. Whereas the prediction based on the four-band model agreed well with the previous experimental results[16,18] on rather wide QW's, it is expected that including the SO bands (fully or as the perturbation) in the model brings about some dependence on the well width and the barrier height for narrow QW's. Actually, Nojima[25] very recently calculated the well-width dependence of the optical-matrix elements in (110) GaAs/(Ga)AlAs QW's, using the 6×6 Kane Hamiltonian, and showed that the in-plane optical anisotropy is pronounced for narrower QW's; Kamada *et al.*[19] suggested the enhancement in in-plane anisotropy for narrower QW's in their experimental study on (110) $In_xGa_{1-x}As_yP_{1-y}$ QW's. However, to our knowledge there has been no systematic experimental report on the well-width dependence of the in-plane optical anisotropy in low-symmetry-plane QW's; the essential physics for the origin of the well-width dependence is still not sufficiently understood.

In this paper we discuss the effects of the SO bands on the polarization properties of interband transitions in QW's. In Sec. II we describe a theoretical formalism used to calculate the optical-matrix element with the effect of the SO bands taken into account. In Sec. III we present calculated results of optical-matrix elements as functions of the well width. We first deal with (001) QW's, comparing the $GaAs/Al_xGa_{1-x}As$ and $Ga_{0.5}In_{0.5}P/(Al_xGa_{1-x})_{0.5}In_{0.5}P$ systems, and then investigate (110) QW's comprising $GaAs/Al_xGa_{1-x}As$. On the other hand, we make a more general discussion of the effect of the SO bands in the Appendix according to a perturbational approach, which is also applicable for other QW's such as (111) and (113) QW's. In Sec. IV we present experimental results of polarized photoluminescence (PL) measurements on (110) $GaAs/Al_{0.2}Ga_{0.8}As$ QW's, and compare them with theoretically calculated results. Finally, the results are summarized in Sec. V.

II. THEORETICAL FORMALISM

We consider electric-dipole interband transitions at the Brillouin-zone center in a (001) or (110) QW. In order to calculate the matrix elements for the electric-dipole transitions, we must first obtain the wave functions of the conduction- and valence-band states, i.e., Ψ_c and Ψ_v. These wave functions can be obtained through solving Schrödinger equations, such as $H_t\Psi_v=E\Psi_v$, with appropriate boundary conditions at the heterointerfaces. In the following we begin with a description of the wave function and the effective-mass Hamiltonian H_t for the valence-band state at the zone center in (001) and (110) QW's in the six-band Luttinger-Kohn model.[26]

A. Zone-center Hamiltonian for the valence-band states

We take the quantization axis z of the angular momenta to be perpendicular to the QW interfaces: $z\|[001]$ for the (001) QW; $z\|[110]$ for the (110) QW. As for the in-plane axes x and y, in the case of a (001) QW it is not important how we define them in the (001) QW plane, since the formalism does not depend on the way of defining the in-plane coordinates owing to the high symmetry of the (001) plane. On the other hand, in the case of a (110) QW it is convenient to take the in-plane axes so as to coincide with some principal axes in the (110) plane. It has been shown that $[\bar{1}10]$ and [001] are the principal axes of the optical-matrix elements (i.e., the principal dielectric axes) for the (110) QW.[18] Therefore, we take the x and y axes to be along $[\bar{1}10]$ and [001], respectively, in the case of a (110) QW.

According to the six-band Luttinger-Kohn model,[26] we take the six bases representing the spin-$\frac{3}{2}$ states as

$$\phi_1(\mathbf{r})=u_{\mathrm{HH}(+)}=|\tfrac{3}{2},\tfrac{3}{2}\rangle=-\frac{1}{\sqrt{2}}|(x+iy)\uparrow\rangle\ , \tag{1a}$$

$$\phi_2(\mathbf{r})=u_{\mathrm{LH}(+)}$$
$$=|\tfrac{3}{2},-\tfrac{1}{2}\rangle=\frac{1}{\sqrt{6}}|(x-iy)\uparrow\rangle+(\tfrac{2}{3})^{1/2}|z\downarrow\rangle\ , \tag{1b}$$

$$\phi_3(\mathbf{r})=u_{\mathrm{SO}(+)}$$
$$=|\tfrac{1}{2},-\tfrac{1}{2}\rangle=-\frac{1}{\sqrt{3}}|(x-iy)\uparrow\rangle+\frac{1}{\sqrt{3}}|z\downarrow\rangle\ , \tag{1c}$$

$$\phi_4(\mathbf{r})=u_{\mathrm{HH}(-)}=|\tfrac{3}{2},-\tfrac{3}{2}\rangle=\frac{1}{\sqrt{2}}|(x-iy)\downarrow\rangle\ , \tag{1d}$$

$$\phi_5(\mathbf{r})=u_{\mathrm{LH}(-)}$$
$$=|\tfrac{3}{2},\tfrac{1}{2}\rangle=-\frac{1}{\sqrt{6}}|(x+iy)\downarrow\rangle+(\tfrac{2}{3})^{1/2}|z\uparrow\rangle\ , \tag{1e}$$

$$\phi_6(\mathbf{r})=u_{\mathrm{SO}(-)}=|\tfrac{1}{2},\tfrac{1}{2}\rangle=\frac{1}{\sqrt{3}}|(x+iy)\downarrow\rangle+\frac{1}{\sqrt{3}}|z\uparrow\rangle\ . \tag{1f}$$

Here the designations x, y, and z refer to the corresponding symmetry properties under operations of the tetrahedral group; $\uparrow$ and $\downarrow$ refer to spin-up and -down, respectively. The zone-center wave function of a valence-band state is expanded in these six basis functions,

$$\Psi_v(\mathbf{r})=\sum_{i=1}^{6} f_i(z)\phi_i(\mathbf{r})\ , \tag{2}$$

where f_i's are envelope functions. The total Hamiltonian for the valence-band state can be written as the sum of the kinetic term and the spin-orbit interaction term:

$$H_t=H_k+H_{\mathrm{SO}}\ . \tag{3}$$

For both (001) and (110) QW's, the 6×6 matrices of these Hamiltonians at the zone center become block diagonal,

$$H_t^{\mathrm{LK}}=\begin{bmatrix} H_t^{\mathrm{LK}(3)} & 0 \\ 0 & H_t^{\mathrm{LK}(3)} \end{bmatrix}$$
$$=\begin{bmatrix} H_k^{\mathrm{LK}(3)} & 0 \\ 0 & H_k^{\mathrm{LK}(3)} \end{bmatrix}+\begin{bmatrix} H_{\mathrm{SO}}^{\mathrm{LK}(3)} & 0 \\ 0 & H_{\mathrm{SO}}^{\mathrm{LK}(3)} \end{bmatrix}\ . \tag{4}$$

Thus each valence-band state is doubly degenerate, and we can set $f_1=f_{\mathrm{HH}}$, $f_2=f_{\mathrm{LH}}$, $f_3=f_{\mathrm{SO}}$, and $f_4=f_5=f_6=0$ for one of the two degenerated states, while $f_4=f_{\mathrm{HH}}$, $f_5=f_{\mathrm{LH}}$, $f_6=f_{\mathrm{SO}}$, and $f_1=f_2=f_3=0$ for the other. Among the two terms in the Hamiltonian, the spin-orbit interaction term is naturally diagonalized, since the eigenstates of the angular momenta are adopted as the basis functions: It is written

$$H_{\mathrm{SO}}^{\mathrm{LK}(3)}=\frac{\Delta}{3}\begin{bmatrix} -1 & 0 & 0 \\ 0 & -1 & 0 \\ 0 & 0 & 2 \end{bmatrix}\ , \tag{5}$$

where Δ is the spin-orbit splitting energy. On the other hand, the 3×3 kinetic Hamiltonian is not diagonal and is written as

$$H_k^{\mathrm{LK}(3)}=\begin{bmatrix} P_k-Q_k & R_k & -\sqrt{2}R_k \\ R_k & P_k+Q_k & \sqrt{2}Q_k \\ -\sqrt{2}R_k & \sqrt{2}Q_k & P_k \end{bmatrix}\ , \tag{6}$$

where

$$P_k=-\gamma_1\left[\frac{\hbar^2}{2m_0}\right]\frac{d^2}{dz^2} \tag{7}$$

for both a (001) and a (110) QW, while Q_k and R_k are different between (001) and (110) QW's. For a (001) QW,

$$Q_k=-2\gamma_2\left[\frac{\hbar^2}{2m_0}\right]\frac{d^2}{dz^2}\ , \tag{8a}$$

$$R_k=0\ ; \tag{9a}$$

for a (110) QW,

$$Q_k=-\left[\frac{1}{2}\gamma_2+\frac{3}{2}\gamma_3\right]\left[\frac{\hbar^2}{2m_0}\right]\frac{d^2}{dz^2}\ , \tag{8b}$$

$$R_k=-\frac{\sqrt{3}}{2}(\gamma_3-\gamma_2)\left[\frac{\hbar^2}{2m_0}\right]\frac{d^2}{dz^2}\ , \tag{9b}$$

where the γ's represent Luttinger parameters. The off-diagonal elements of the kinetic Hamiltonian cause the mixing between the spin-$\frac{3}{2}$ basis functions. In the case of a (001) QW, only the bulk light-hole states $u_{\mathrm{LH}(\pm)}$ are mixed with the SO-band states $u_{\mathrm{SO}(\pm)}$ to form light-hole states in a QW, leaving the bulk heavy-hole states $u_{\mathrm{HH}(\pm)}$ decoupled, since $R_k=0$. On the other hand, u_{HH}, u_{LH}, and u_{SO} are mixed to form any confined hole states in a (110) QW, i.e., not only the light-hole states but also the heavy-hole states in a (110) QW are coupled to the SO-band states. (This situation is rather similar to the case of quantum wires. Citrin and Chang[27] discussed the effect of SO bands in quantum wires, and have pointed out that both heavy- and light-hole states at the zone center in quantum wires are coupled to the SO bands.)

B. Optical-matrix elements

Regarding the conduction-band states, the wave function at the zone center can be written as

$$\Psi_{c(\pm)}(\mathbf{r})=f_c(z)u_{c(\pm)}(\mathbf{r})\ , \tag{10}$$

where $f_c(z)$ is an envelope function and $u_{c(\pm)}$ is the cell-periodic part of the Bloch function for the conduction band. The cell-periodic part can be written $u_{c(+)}=|s\uparrow\rangle|\frac{1}{2},+\frac{1}{2}\rangle$ or $u_{c(-)}=|s\downarrow\rangle=|\frac{1}{2},-\frac{1}{2}\rangle$, where the designation s refers to the s-like symmetry property under operations of the tetrahedral group. The conduction-band envelope function $f_c(z)$ can be obtained within the particle-in-the-box model.

Using the zone-center wave functions of conduction- and valence-band states, the optical-matrix element at the zone center can be written

$$|\hat{\mathbf{e}}\cdot\mathbf{M}|^2=\sum_{\sigma=\pm}|\langle\Psi_{c(\sigma)}|\hat{\mathbf{e}}\cdot\mathbf{p}|\Psi_v\rangle|^2\ , \tag{11}$$

where $\hat{\mathbf{e}}$ is a unit vector denoting the polarization direction of the light, and $\mathbf{p}$ is the momentum operator. After a simple calculation, Eq. (11) can be written more explicitly as

$$|M_x|^2=\left|\frac{1}{\sqrt{2}}I_{c\mathrm{HH}}-\frac{1}{\sqrt{6}}I_{c\mathrm{LH}}+\frac{1}{\sqrt{3}}I_{c\mathrm{SO}}\right|^2P^2 , \quad (12a)$$

$$|M_y|^2=\left|\frac{1}{\sqrt{2}}I_{c\mathrm{HH}}+\frac{1}{\sqrt{6}}I_{c\mathrm{LH}}-\frac{1}{\sqrt{3}}I_{c\mathrm{SO}}\right|^2P^2 , \quad (12b)$$

$$|M_z|^2=\left|\frac{2}{\sqrt{6}}I_{c\mathrm{LH}}+\frac{1}{\sqrt{3}}I_{c\mathrm{SO}}\right|^2P^2 , \quad (12c)$$

where we have written $|\langle s|p_x|x\rangle|=|\langle s|p_y|y\rangle|=|\langle s|p_z|z\rangle|=P$, and have defined the overlap integrals $I_{c\mathrm{HH}}$, $I_{c\mathrm{LH}}$, and $I_{c\mathrm{SO}}$ as

$$I_{c\mathrm{HH}}=\int f_c(z)f_{\mathrm{HH}}(z)dz , \quad (13a)$$

$$I_{c\mathrm{LH}}=\int f_c(z)f_{\mathrm{LH}}(z)dz , \quad (13b)$$

$$I_{c\mathrm{SO}}=\int f_c(z)f_{\mathrm{SO}}(z)dz . \quad (13c)$$

The effects due to the terms related to $I_{c\mathrm{SO}}$ in Eqs. (12a)–(12c) can be referred to as the effects of the SO band on the optical-matrix elements.

The above representation of the optical-matrix elements can still be simplified for a (001) QW, since the heavy-hole state is decoupled from the other hole states. For the heavy-hole transition, therefore, the overlap integrals $I_{c\mathrm{LH}}$ and $I_{c\mathrm{SO}}$ are both zero; the optical-matrix elements are derived only from $I_{c\mathrm{HH}}$ for the heavy-hole transition. On the other hand, the optical-matrix elements for the light-hole transition are calculated as

$$|M_x|^2=|M_y|^2=\left|\frac{1}{\sqrt{6}}I_{c\mathrm{LH}}-\frac{1}{\sqrt{3}}I_{c\mathrm{SO}}\right|^2P^2 , \quad (14a)$$

$$|M_z|^2=\left|\frac{2}{\sqrt{6}}I_{c\mathrm{LH}}+\frac{1}{\sqrt{3}}I_{c\mathrm{SO}}\right|^2P^2 . \quad (14b)$$

In a (001) QW, therefore, the effect of the SO band appears only in the light-hole transitions, and does not appear in the heavy-hole transitions at the zone center. As is clear from Eqs. (14a) and (14b), when the effect of the SO band is included, the in-plane matrix element $|M_x|^2=|M_y|^2$ becomes smaller, while $|M_z|^2$ becomes larger than those calculated within the model neglecting the SO band, if $I_{c\mathrm{SO}}$ has the same sign as $I_{c\mathrm{LH}}$. On the other hand, if $I_{c\mathrm{SO}}$ has the opposite sign to $I_{c\mathrm{LH}}$, the reverse occurs. The latter is revealed in Sec. III to be actually true, by illustrating the calculated results for the light-hole transition in practically important QW's; it is proven more generally by adopting a perturbational approach in the Appendix.

As to the heavy-hole transition in a (110) QW, it has been shown[28] that $I_{c\mathrm{LH}}$ has a small but finite value with a sign opposite to $I_{c\mathrm{HH}}$. In the model neglecting the SO band, therefore, $|M_x|^2$ has been calculated to be slightly larger than $|M_y|^2$ for the heavy-hole transition.[28] This in-plane anisotropy is enlarged by the inclusion of SO bands into the calculation, as is clear from Eqs. (12a) and (12b), if $I_{c\mathrm{SO}}$ has the same sign as $I_{c\mathrm{HH}}$. This is also shown to be true in a perturbational approach in the Appendix, as well as by calculated results in Sec. III.

III. RESULTS OF CALCULATION

Here we present calculated results regarding the well-width dependence of the optical-matrix elements with the effect of the SO band taken into account. In the calculation, we have used the exact form of the solution of the coupled effective-mass equations for the valence-band state, equations which are represented using the 3×3 Hamiltonian defined in Sec. II.

In previous studies on (110) QW's, Gershoni *et al.*[17] as well as Nojima[25] calculated valence-band wave functions on the basis of multiband effective-mass approximations including the SO bands. In either of the two previous studies, the envelope functions were expanded using an orthonormal function set in order to solve the coupled effective-mass equations. Then approximate wave functions were obtained there in series-expansion forms in which an infinite series of the orthonormal functions was truncated practically. On the other hand, simple analytical forms of the envelope functions were obtained in this study as an exact solution of the coupled effective-mass equations. The method for solving the coupled effective-mass equations exactly, which is essentially similar to the method described in a previous paper by the author,[28] is described in detail in Ref. 29.

The calculated results of the optical-matrix elements are presented in the following for (001) QW's as well as (110) QW's. As for (110) QW's, we deal with two material systems. First, we consider (001) $GaAs/Al_xGa_{1-x}As$ QW's; as the second example of (001) QW's, we deal with $Ga_{0.5}In_{0.5}P/(Al_xGa_{1-x})_{0.5}In_{0.5}P$ QW's. The latter system is a system lattice matched to the GaAs substrate, and is now receiving much attention as a material system for laser diodes operating in the 600-nm range. In this system the effects of the SO bands are expected to play a more important role than in the $GaAs/Al_xGa_{1-x}As$ system, since the spin-orbit splitting energy Δ is much smaller (Δ is 340 meV for GaAs while 95 meV for $Ga_{0.5}In_{0.5}P$). Lastly, we deal with (110) $GaAs/Al_xGa_{1-x}As$ QW's as an example of (110) QW's.

TABLE I. Luttinger parameters and spin-orbit splitting energies used in the calculations. Values for Luttinger parameters are taken from Ref. 30, while those for spin-orbit splitting energy are from Ref. 31.

	γ_1	γ_2	γ_3	Δ (meV)
GaAs	7.65	2.41	3.28	0.34
AlAs	4.04	0.78	1.57	0.28
InP	6.28	2.08	2.76	0.11
GaP	4.20	0.98	1.66	0.08
AlP	3.47	0.06	1.15	0.07

The material constants used in the calculation for $GaAs/Al_xGa_{1-x}As$ and $Ga_{0.5}In_{0.5}P/(Al_xGa_{1-x})_{0.5}In_{0.5}P$ QW's were as follows. As the valence-band parameters for binary compounds, Luttinger parameters and spin-orbit splitting energies were taken from Lawaetz[30] and Krijn,[31] respectively, and are listed in Table I. The parameters for alloyed materials were obtained by a linear interpolation between the values for binary compounds. As for the effective masses of electrons, we set $m_e^*=(0.067+0.083x)m_0$ for $Al_xGa_{1-x}As$ and $m_e^*=(0.11+0.86x)m_0$ for $(Al_xGa_{1-x})_{0.5}In_{0.5}P$.[32] The total band-gap differences at the heterointerfaces were taken to be $\Delta E_g=1.185x+0.37x^2$ (eV) for the $GaAs/Al_xGa_{1-x}As$ system and $\Delta E_g=0.521x$ (eV) for the $In_{0.5}Ga_{0.5}P/(Al_xGa_{1-x})_{0.5}In_{0.5}P$ system.[32] The conduction-band-offset ratio $R_c=V_c/\Delta E_g$ was set to be 0.67 for the former system while 0.43 for the latter.[33] The offset ratio for the $GaAs/Al_xGa_{1-x}As$ system was assumed to be independent of the orientation of the heterointerface.[34]

Figures 1(a) and 1(b) show the calculated results of the squared optical-matrix elements for the first-conduction-to-first-light-hole-state ($c1-1h1$) transition in (001) $GaAs/Al_xGa_{1-x}As$ QW's as functions of the well width. Figure 1 (a) shows the matrix elements for the z polarization, while Fig. 1(b) shows those for the in-plane polarization. The values were normalized by the squared optical-matrix element for the bulk material, $|M_b|^2=\frac{1}{3}P^2$. Figure 2 shows the ratio of $|M_z|^2$ to $|M_x|^2$ as a function of the well width. In those figures, the calculated results assuming the infinite height of the barrier potential are also plotted by dotted lines, together with solid lines which represent results calculated for GaAs wells sandwiched by finite barriers of $Al_{0.3}Ga_{0.7}As$ or AlAs.

In the wide-well limit the values of the normalized matrix elements $|M_z|^2/|M_b|^2$ and $|M_x|^2/|M_b|^2$ approach 2.0 and 0.5, respectively, being independent of the height of the barrier potential, as can be seen in Figs. 1(a) and 1(b). As a result, the ratio between them approaches $|M_z|^2:|M_x|^2=4:1$, as can be seen in Fig. 2. This ratio is well known as the ratio of the squared matrix elements between the TM and TE modes, which is obtained within the approximation of neglecting the coupling to the SO band. When the well width is decreased, the behavior of the matrix elements is different, depending on the barrier height.

It is interesting to direct our attention first to the case of the infinitely high barriers shown by the dotted lines. As the well width is decreased, $|M_z|^2$ decreases, while $|M_x|^2$ increases; thus the ratio $|M_z|^2/|M_x|^2$ decreases. (Note here that the sum rule, i.e., $|M_x|^2+|M_y|^2+|M_z|^2=2|M_x|^2+|M_z|^2=3|M_b|^2$, is satisfied for the entire well-width range in the case of an infinite barrier height.) In the narrow-well limit, $|M_z|^2/|M_b|^2$ and $|M_x|^2/|M_b|^2$ approach 0 and 1.5, respectively. These values in the limit are coincident with the values for the heavy-hole transition. This is because the light-hole state degenerates with the heavy-hole state in a (001) QW in the limit of the zero width within the infinitely high-barrier model. (In this limit the kinetic term becomes so large that the spin-orbit interaction term can be neglected. Among the three eigenstates of the kinetic Hamiltonian $H_k^{LK(3)}$, one is nondegenerate while the other two are degenerate. This degeneracy corresponds to the degeneracy between heavy- and light-hole states in the zero-width limit.)

On the other hand, the changes in the cases of actual QW's with $Al_xGa_{1-x}As$ finite barriers are not so drastic as in the case of an infinite barrier; $|M_z|^2/|M_b|^2$ does not

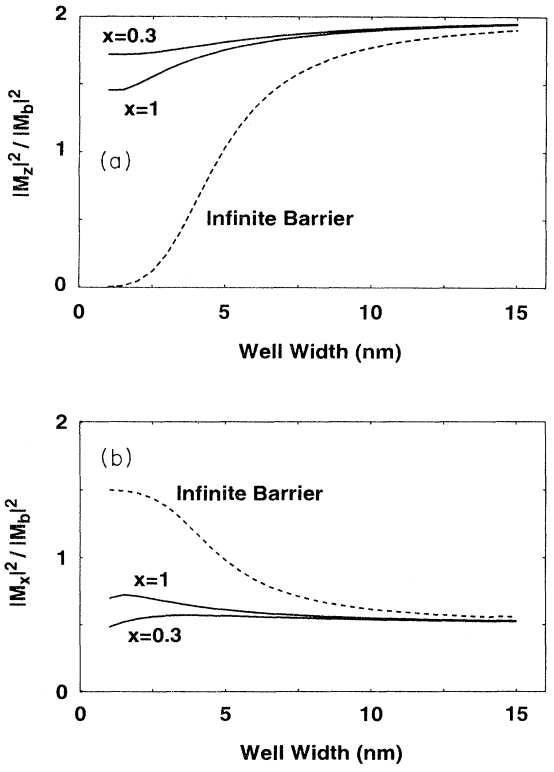

FIG. 1. Squared optical-matrix elements for the $c1$-lh1 transition in (001) $GaAs/Al_xGa_{1-x}As$ QW's as a function of the well width. (a) $|M_z|^2/|M_b|^2$, (b) $|M_x|^2/|M_b|^2$.

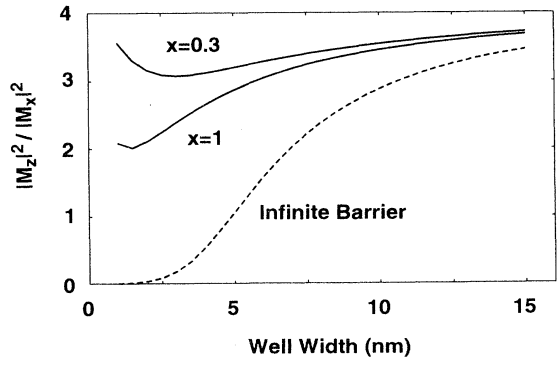

FIG. 2. Ratio of squared optical-matrix elements $|M_z|^2/|M_x|^2$ for the $c1$-lh1 transition in (001) $GaAs/Al_xGa_{1-x}As$ QW's as a function of the well width.

decrease less than 1.5 and $|M_x|^2/|M_b|^2$ does not increase more than 0.75 for the highest actual barrier of AlAs, as can be seen in Figs. 1(a) and 1(b). Therefore, neglecting the coupling to the SO bands can be regarded as being a good approximation for (001) $GaAs/Al_xGa_{1-x}As$ QW's, especially for low values of the Al content x. It is thus deduced that the ratio $|M_z|^2/|M_x|^2$ in a QW with low-Al-content barriers is not so far from 4, being independent of the well width, as can be seen in Fig. 2. Actually, Sonek *et al.*[35] experimentally obtained a value of 3.8 as the ratio of TM absorption to TE in a (001) $GaAs/Al_xGa_{1-x}As$ QW with $x=0.26$ and a well width of 8 nm. However, one should remember that for narrow wells with high-Al-content barriers the ratio $|M_z|^2/|M_x|^2$ decreases to be as small as 2.

The effects of the SO bands become more pronounced when the spin-orbit splitting energy of the well-layer material is small. Figures 3(a) and 3(b) show the calculated results of $|M_z|^2/|M_b|^2$ and $|M_x|^2/|M_b|^2$, respectively, for the $c1$-lh1 transition in (001) $Ga_{0.5}In_{0.5}P/(Al_xGa_{1-x})_{0.5}In_{0.5}P$ QW's. Comparing Figs. 3(a) and 3(b) with Figs. 1(a) and 1(b), one can see that the well-width dependence is more pronounced in $Ga_{0.5}In_{0.5}P$ QW's than in GaAs QW's. For finite barrier heights, $|M_z|^2/|M_b|^2$ decreases with decreasing well width, reaches a minimum, and then increases. $|M_x|^2/|M_b|^2$ shows the opposite behavior. For the case of $x=1$, $|M_z|^2/|M_b|^2$ reaches almost to 0.5; $|M_x|^2/|M_b|^2$ exceeds 1.0. Those values are about one-fourth and twice the values calculated within the model neglecting the SO band, respectively. Thus the model neglecting the SO band cannot stand at all for the light-hole transition in $Ga_{0.5}In_{0.5}P$ QW's with high barrier heights and narrow well widths. The increase of $|M_z|^2$ after reaching the minimum and the decrease of $|M_x|^2$ after reaching the maximum for very narrow well widths are both due to the wave-function overflow out of the well by narrowing the well width.[25] Figure 4 shows the ratio of $|M_z|^2$ to $|M_x|^2$ for (001) $Ga_{0.5}In_{0.5}P/(Al_xGa_{1-x})_{0.5}In_{0.5}P$ QW's as a function of the well width. The ratio is evidently smaller than the calculated value within the model neglecting the SO band, even at a rather wide-well width of 15 nm. The ratio becomes even smaller with decreasing well width, and reaches the minimum at a well width of 2–3 nm. When $x=1$, the ratio becomes less than 1 for well widths narrower than 3.5 nm, i.e., the light-hole transition probability is larger for the TE mode than for the TM mode. Thus the reversal in the TE/TM ratio occurs for the light-hole transition in narrow (001) $Ga_{0.5}In_{0.5}P/Al_{0.5}In_{0.5}P$ QW's.

Next we turn to the case of (110) QW's. In (110) QW's, not only the light-hole states but also the heavy-hole states are mixed with the SO bands. For the heavy-hole transition, the optical-matrix element for z polarization remains very small and almost negligible, even when the SO bands are taken into account. We therefore concentrate on the optical-matrix elements of the heavy-hole transition only for in-plane polarization.

Figure 5 shows the relative matrix elements for the first-conduction-to-first-heavy-hole-state ($c1$-hh1) transition in (110) $GaAs/Al_xGa_{1-x}As$ QW's as functions of the well width, for in-plane polarizations, i.e., x and y polarizations, which were calculated with the effect of the SO bands taken into account. In Fig. 5, the solid lines correspond to the finite-barrier-height cases, while the dotted lines correspond to the infinite-barrier-height case. Among the in-plane polarizations, the matrix elements are different for x and y polarizations. Figure 6 shows the in-plane polarization degree, which is defined as $P_{\text{in-plane}}=(|M_x|^2-|M_y|^2)/(|M_x|^2+|M_y|^2)$, as a function of the well width. The solid curves indicate the calculated results with the effect of the SO bands taken into ac-

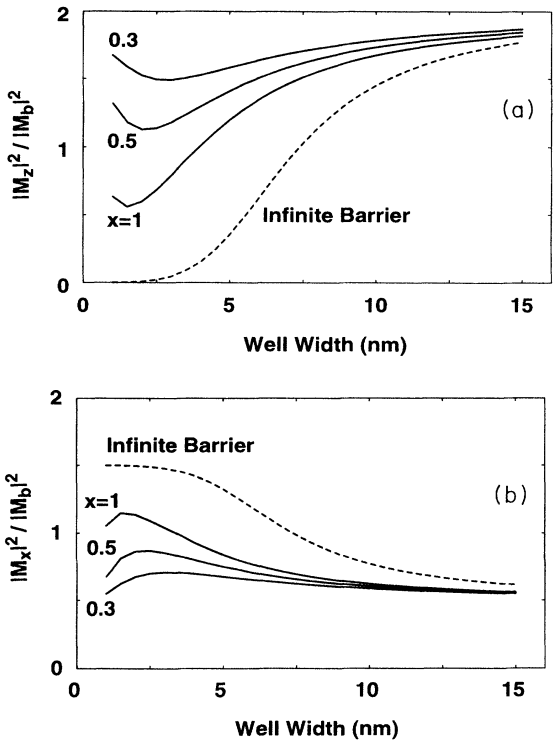

FIG. 3. Squared optical-matrix elements for the $c1$-lh1 transition in (001) $Ga_{0.5}In_{0.5}P/(Al_xGa_{1-x})_{0.5}In_{0.5}P$ QW's as a function of the well width. (a) $|M_z|^2/|M_b|^2$, (b) $|M_x|^2/|M_b|^2$.

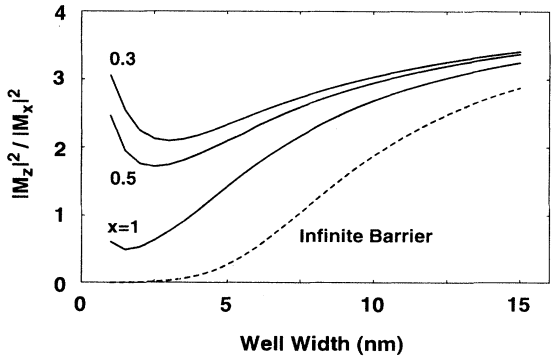

FIG. 4. Ratio of squared optical-matrix elements $|M_z|^2/|M_x|^2$ for the $c1$-lh1 transition in (001) $Ga_{0.5}In_{0.5}P/(Al_xGa_{1-x})_{0.5}In_{0.5}P$ QW's as a function of the well width.

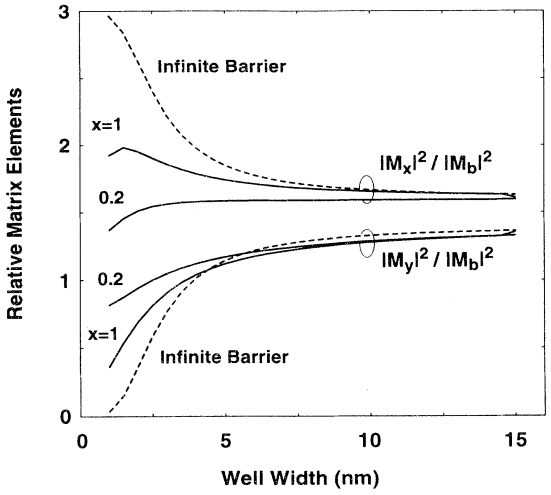

FIG. 5. Squared in-plane optical-matrix elements for the $c1$-hh1 transition in (110) GaAs/$Al_xGa_{1-x}As$ QW's as a function of the well width.

count for QW's with $Al_xGa_{1-x}As$ barriers with $x=1$ or 0.2, while the dashed curve indicates those for QW's with infinitely high barriers. In this figure the calculated results without the effect of the SO bands[16] are also plotted by the dash-dotted line, which result in a constant value being independent of the well width.

In the wide-well limit, the values of the normalized matrix elements ($|M_x|^2/|M_b|^2$ and $|M_y|^2/|M_b|^2$) and the in-plane polarization degree approach the values calculated without the SO bands in Ref. 16, being irrelevant to the height of the barrier potential, as can be seen in Figs. 5 and 6. When the well width is decreased in the case of an infinite barrier height, $|M_x|^2/|M_b|^2$ increases to reach 3 in the zero-width limit, while $|M_y|^2/|M_b|^2$ decreases to vanish, as indicated by the dotted lines. As a result, the in-plane polarization degree increases with decreasing well width to reach 100% in the zero-width limit for the infinite barrier height, as shown by the dotted line in Fig. 6. [This means that the heavy-hole state in a (110) QW has only the $|x\rangle$ component in the limit of the zero width. In this limit the kinetic Hamiltonian H_k is so large that the spin-orbit interaction Hamiltonian H_{SO} can be neglected. Note here that H_k is diagonalized in the ($|x\rangle$, $|y\rangle$, $|z\rangle$) basis set. While the $|x\rangle$ and $|y\rangle$ states degenerate in a (001) QW, they do not degenerate in a (110) QW owing to the low symmetry. Then the lowest-energy eigenstate $|x\rangle$ of H_k corresponds to the heavy-hole state in a (110) QW in the zero-width limit, while the second-lowest-energy eigenstate $|y\rangle$ corresponds to the light-hole state.] For finite barrier heights, the well-width dependence is more moderate. The decrease of $|M_x|^2$ for very narrow well widths, which can be seen in Fig. 5, is due to the wave-function overflow out of the well by narrowing the well width.[25] In Sec. IV, these calculated results regarding the well-width dependence of the in-plane polarization degree are compared with the experimental results for (110) GaAs/$Al_{0.2}Ga_{0.8}As$ QW's.

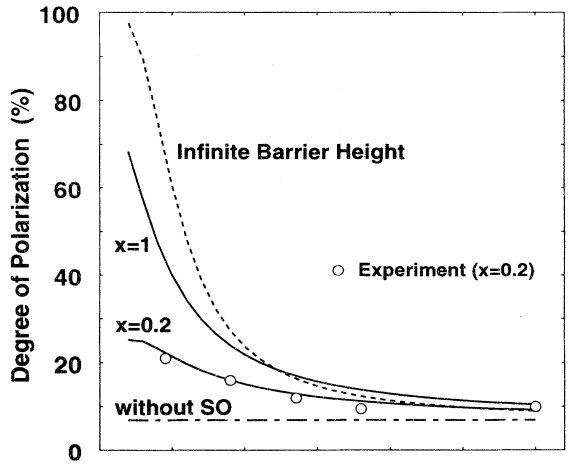

FIG. 6. In-plane polarization degree, $P_{\text{in-plane}}=(|M_x|^2-|M_y|^2)/(|M_x|^2+|M_y|^2)$, for the $c1$-hh1 transition in (110) GaAs/$Al_xGa_{1-x}As$ QW's as a function of the well width, which were calculated with the effect of the SO bands taken into account (solid and dashed curves). The dash-dotted line shows the calculated result without the SO bands. Open circles indicate the degree of polarization at the peak wavelength of PL from (110) GaAs/$Al_{0.2}Ga_{0.8}As$ QW's.

IV. EXPERIMENTAL STUDY ON (110) GaAs/$Al_{0.2}Ga_{0.8}As$ QW's AND COMPARISON WITH THEORY

In this section we describe the experimental study regarding the in-plane optical anisotropy of the heavy-hole excitonic transition in (110) GaAs/$Al_{0.2}Ga_{0.8}As$ QW's by means of a PL method. The samples used in this study were grown by molecular-beam epitaxy (MBE) on a (110)-oriented n^+-GaAs substrate. The growth conditions were described in detail in our previous paper.[16] In short, the growth conditions were as follows. The substrates used were (110) misoriented by 6° toward the nearest (111)A plane; the growth temperature was 590 °C; the growth rate was 0.45 μm/h for GaAs; the beam-equivalent ion-gauge pressure of As_4 was 1.5×10^{-4} Torr at the substrate position. These growth conditions, i.e., the low growth temperature, the slow growth rate, and the high As_4 pressure, were chosen so as to obtain a smooth surface.

Three samples were investigated in this study. One was the same as that used in our previous paper,[16] which had a positive-intrinsic-negative (p-i-n) structure with a multiple-QW structure embedded in the middle of the i layer. The multiple-QW structure comprised 20 periods of alternating 9-nm GaAs wells and 13.5-nm $Al_xGa_{1-x}As$ barriers. The other two samples comprised i layers only. One had a single QW with a well width of 15 nm. The last sample had four QW's with different well widths, i.e., 9, 6.75, 4.5, and 2.25 nm, which were separated from each other by 50-nm-thick $Al_xGa_{1-x}As$ barrier layers. The Al contents of the $Al_xGa_{1-x}As$ bar-

rier layers in the above-mentioned samples were all 0.2.

The polarized PL spectra were taken at 77 K in the conventional way by setting a linear polarizer in front of the monochromator. The 488-nm line of an Ar-ion laser was used as the excitation source, and the exciting light was about 20° off normal incidence. The sample was set so that its $[1\bar{1}1]$ axis became vertical. Thus, both the $[1\bar{1}0]$ and [001] axes made an angle of 45° with the slit of the monochromator. The backscattered luminescence light was detected normal to the surface. The spectra were taken for the two orthogonal polarizations, i.e., $[\bar{1}10]$ and [001] polarizations. Since the $[\bar{1}10]$ and [001] polarization directions are mirror symmetrical with respect to the vertical plane, it was not necessary to correct for the luminescence intensity of those polarization directions for the polarization dependence of the grating.

Figure 7 shows the PL spectra from a sample including a multiple-QW structure with a well width of 9 nm, where the solid line shows the spectrum for the $[\bar{1}10]$ polarization, while the dashed line shows that for the [001] polarization. Although the peak in the PL spectra appears at a longer wavelength by 3 nm than the heavy-hole excitonic peak in the photocurrent spectra in our previous study,[16] we also attributed the peak to the heavy-hole excitons in the PL spectra. The rather large Stokes shift suggests a fluctuation in the well width and the Al content of the barrier layers, which is consistent with the rather large half-width of the PL peak.

We confirmed that, although the excitation light was linearly polarized, the intensity ratio between the two polarized components of the luminescence, $I_{[\bar{1}10]}$ and $I_{[001]}$, was irrelevant to the polarization direction of the excitation light. The degree of polarization, which is defined as $(I_{[\bar{1}10]}-I_{[001]})/(I_{[\bar{1}10]}+I_{[001]})$, is also plotted in Fig. 7 as a function of the wavelength. The polarization degree (including the sign) at the peak wavelength of the heavy-hole transition derived from the PL spectra in the present study was 9%, and is in good agreement with that derived from the photocurrent spectra in our previous study.[16] We therefore conclude that the polarization degree derived from the PL spectra, as well as that derived from the photocurrent spectra, directly corresponds to the polarization degree for the heavy-hole excitonic transition, if the excitation energy is sufficiently high compared with the band gap of the barrier layer.

One can see in Fig. 7 that the degree of polarization is almost constant for wavelengths longer than 800 nm, while it decreases to zero when the wavelength is decreased from 800 to 795 nm. In our previous study[16] we observed the absorption peak due to the light-hole excitonic transition appearing at a shorter wavelength by about 10 nm than the heavy-hole excitonic peak in the photocurrent spectra. We then observed that the polarization of the light-hole excitonic transition is opposite to that of the heavy-hole excitonic transition. Furthermore, it is well known that not only the heavy-hole but also the light-hole excitonic emission is observed in the 77-K PL spectrum for a (001) or (111) QW having a well width of 9 nm or wider.[36] Also in this PL spectrum for the (110) QW with a well width of 9 nm, although the light-hole excitonic emission is expected to emerge, it is thought to be unresolved from the heavy-hole excitonic peak due to the broad width of the latter peak. We therefore attributed the decrease in the degree of polarization around a wavelength shorter than the heavy-hole excitonic emission peak by about 10 nm to compensation by the light-hole excitonic emission.

Figure 8 shows the PL spectra for the two orthogonal polarization directions from a sample including a single QW with a well width of 15 nm, together with the degree of polarization. As can be seen in Fig. 8, the polarization degree is almost constant above the peak wavelength of the PL intensity, just as in the 9-nm-wide QW, while it decreases with decreasing wavelength to become negative at wavelengths below 814 nm. The light-hole excitonic

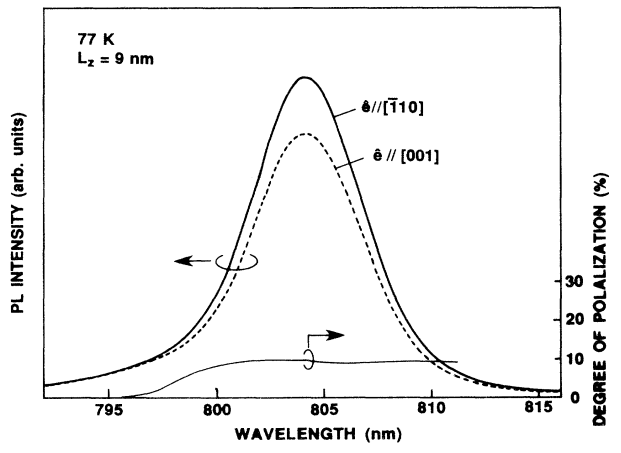

FIG. 7. 77-K PL spectra of a multiple $GaAs/Al_xGa_{1-x}As$ QW structure having a well width of 9 nm. The solid and dashed curves indicate the luminescence components of the $[\bar{1}10]$ and [001] polarizations, respectively. The degree of polarization $P_{\text{in-plane}}=(I_{[\bar{1}10]}-I_{[001]})/(I_{[\bar{1}10]}+I_{[001]})$ is also shown as a function of the wavelength.

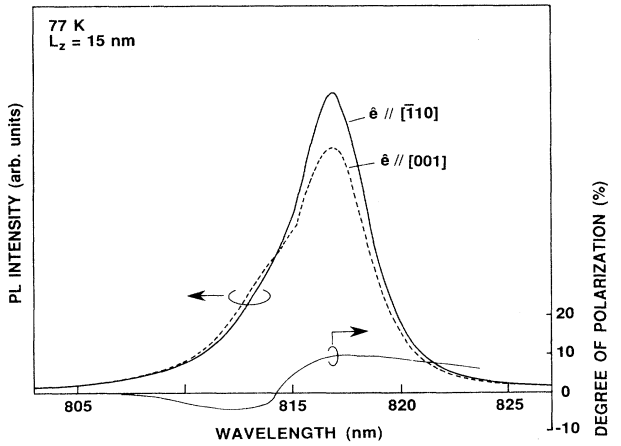

FIG. 8. As in Fig. 7, but for a single-QW structure having a well width of 15 nm.

emission is thought to be more enhanced in the 15-nm-wide QW than in the 9-nm-wide QW due to the smaller separation between the heavy- and light-hole levels. Therefore, the reversal of the polarization degree in sign below 814 nm can reasonably be attributed to the appearance of a light-hole excitonic emission in this wavelength range. The asymmetry of the luminescence peak, which is more enhanced in the [001] spectrum, proves the existence of an unresolved peak of the light-hole excitonic peak.

Thus the degree of polarization in the wavelength range of the light-hole excitonic emission is thought to vary with the well width according to the change in the extent of overlapping with the heavy-hole excitonic emission. On the other hand, the degree of polarization at the peak wavelength for the heavy-hole excitonic emission is thought not to be affected by the overlapping with the light-hole excitonic emission, at least for well widths narrower than 9 nm, since the polarization degree is almost constant around the peak wavelength within the ±5-nm range for the 9-nm-wide QW.

As can be seen from a comparison between Figs. 7 and 8, the degree of polarization in the peak wavelength remained almost unchanged for QW's having well widths of 9 and 15 nm, and was about 9% for either case. This indicates that the polarization degree of the heavy-hole transition does not depend on the well width so much when the well width is wider than 9 nm.

Figure 9 shows the PL spectra for the two polarization directions from a sample including four QW's with different well widths of 9, 6.75, 4.5, and 2.25 nm. One can see a tendency to increase the degree of polarization with decreasing wavelength. (The dashed-dotted line in Fig. 9 is plotted only as a guide to the eye, joining the peaks of the curve for the polarization degree by a straight line.)

In Fig. 6, the degree of polarization at the peak of the PL spectrum is plotted as a function of the well width for the corresponding QW by open circles. It can be seen in Fig. 6 that the degree of polarization increases to be beyond 20% for a well width of 2.25 nm, which value is more than twice as large as the value for a 9-nm QW. We now compare the experimental results with the theoretically calculated results, assuming that the in-plane anisotropy in the squared optical-matrix element calculated in Sec. III dominates the degree of polarization in the heavy-hole excitonic emission in PL. As can be seen in Fig. 6, the experimental results are in good agreement with the calculated results for the $Al_xGa_{1-x}As$ barrier layers with $x=0.2$ when the effect of the SO bands is taken into account. Thus the observed increase in the degree of polarization with decreasing well width is well explained as being due to an increase in the effect of the coupling to the SO bands in the optical-matrix element.

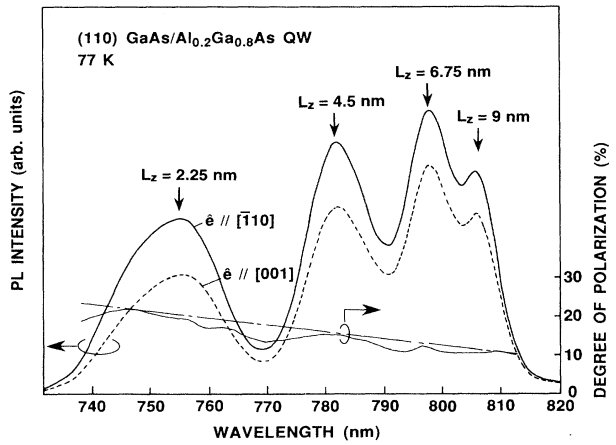

FIG. 9. As in Fig. 7, but for a sample including four single QW's having well widths of 9, 6.75, 4.5, and 2.25 nm, respectively.

V. CONCLUSIONS

We have investigated the effect of the SO bands on the optical-matrix elements in (001) and (110) QW's. The calculated results were shown for (001) $GaAs/Al_xGa_{1-x}As$ and $Ga_{0.5}In_{0.5}P/(Al_xGa_{1-x})_{0.5}In_{0.5}P$ QW's as well as for (110) $GaAs/Al_xGa_{1-x}As$ QW's. The calculated results on the (001) QW's have indicated that, while neglecting the SO bands is a rather good approximation for $GaAs/Al_xGa_{1-x}As$ QW's, it does not stand any more for the light-hole transition in $Ga_{0.5}In_{0.5}P/(Al_xGa_{1-x})_{0.5}In_{0.5}P$ QW's in which the spin-orbit splitting energy is small. The optical-matrix elements in (001) $Ga_{0.5}In_{0.5}P/(Al_xGa_{1-x})_{0.5}In_{0.5}P$ QW's showed an evident dependence on the well width. As the results, the values were found to differ from the conventional prediction by the four-band model, especially for narrow and deep wells, to show the reversal in TM/TE ratio. While in this paper we dealt with only the $Ga_xIn_{1-x}P$ QW's with $x=0.5$, which lattice match to the GaAs substrate, it is expected that the effect of the SO bands on the polarization property is still enhanced owing to the strain effect for lattice-mismatched $Ga_xIn_{1-x}P$ QW's with x other than 0.5.

As for (110) $GaAs/Al_xGa_{1-x}As$ QW's, the effect of the coupling to the SO bands can be seen not only on the light-hole transitions but also on the heavy-hole transitions. The calculated results have indicated that the in-plane optical anisotropy in (110) QW's increases with decreasing well width according to the increase in coupling to the SO bands.

We have also experimentally investigated the well-width dependence of the polarization anisotropy of the heavy-hole excitonic transition in (110) $GaAs/Al_{0.2}Ga_{0.8}As$ QW's having well widths ranging from 2.25 to 15 nm by means of 77-K PL measurements. The evident increase in the degree of polarization has been found for the heavy-hole excitonic emission from QW's narrower than about 7 nm. The experimental results showed good agreement with the calculated results in the model, in which the effect of the coupling to the SO bands is taken into account.

ACKNOWLEDGMENT

The author would like to thank Dr. Masayuki Hata of Sanyo Electric Co., Ltd. for helpful discussions.

APPENDIX: PERTURBATIONAL APPROACH IN INFINITELY HIGH-BARRIER MODEL

In this appendix we discuss the effect of the SO bands on the optical-matrix elements on the basis of a perturbational theory. For simplicity we assume infinitely high barriers. In the infinitely high-barrier model, the envelope functions become simple sinusoidal waves. For example, when we set $z=0$ at an end of the well, the wave function of the nth heavy-hole state can be written as

$$\Psi_{\mathrm{hh}n(+)}=\sum_{i=1}^{3} a_i^{\mathrm{hh}}\left[\frac{2}{L}\right]^{1/2}\sin\left[\frac{n\pi z}{L}\right]\phi_i = \left[\frac{2}{L}\right]^{1/2}\sin\left[\frac{n\pi z}{L}\right]|\mathrm{hh}(+)\rangle\ , \tag{A1}$$

where L is the well width and we have written the cell-periodic part of the heavy-hole wave function as

$$|\mathrm{hh}(+)\rangle=\sum_{i=1}^{3} a_i^{\mathrm{hh}}\phi_i\ . \tag{A2}$$

The cell-periodic part of the light-hole wave function $|\mathrm{lh}(+)\rangle$ is defined in a similar manner. Then, d^2/dz^2 in P_k, Q_k, and R_k can be replaced by $-\pi^2/L^2$. The optical-matrix elements can be calculated using only the cell-periodic parts of the wave functions. For example, the matrix element for the heavy-hole transition can be written as

$$|\hat{\mathbf{e}}\cdot\mathbf{M}|^2=|\langle s\uparrow|\hat{\mathbf{e}}\cdot\mathbf{p}|\mathrm{hh}(+)\rangle|^2+|\langle s\downarrow|\hat{\mathbf{e}}\cdot\mathbf{p}|\mathrm{hh}(+)\rangle|^2\ . \tag{A3}$$

In the following we derive the cell-periodic parts of the hole wave functions, $|\mathrm{hh}(+)\rangle$ and $|\mathrm{lh}(+)\rangle$, on the basis of perturbation theory, in which we treat H_{SO} as the unperturbed Hamiltonian and H_k as the perturbation, and calculate the optical-matrix elements according to Eq. (A3).

1. (001) QW

As mentioned in Sec. II, the heavy-hole state in a (001) QW is not affected by the perturbation due to the coupling of the SO band through H_k. Therefore, we discuss only the light-hole state. Within the first-order perturbation, the cell-periodic part of the wave function of the light-hole state can be written as

$$|\mathrm{lh}(+)\rangle_{1\mathrm{st}}=|\tfrac{3}{2},-\tfrac{1}{2}\rangle-\frac{\sqrt{2}Q_k}{\Delta-Q_k}|\tfrac{1}{2},-\tfrac{1}{2}\rangle\ . \tag{A4}$$

Using this perturbed wave function and Eqs. (14a) and (14b), the optical-matrix element for the light-hole transition can be written as

$$|M_x|^2=|M_y|^2=\left[1+\frac{2Q_k}{\Delta-Q_k}\right]^2\frac{P^2}{6}\ , \tag{A5a}$$

$$|M_z|^2=\left[1-\frac{Q_k}{\Delta-Q_k}\right]^2\frac{2}{3}P^2\ . \tag{A5b}$$

From the above representations, it can be deduced that the conventional prediction by the four-band Luttinger-Kohn model is recovered in the wide-well limit. However, the squared in-plane matrix elements, $|M_x|^2$ and $|M_y|^2$, increase as the well width decreases, while $|M_z|^2$ decreases as the well width decreases, since Q_k is larger for a narrower well. Thus the ratio of $|M_z|^2$ to the squared in-plane optical-matrix element decreases from the value of 4 for the wide-well limit when the well width decreases. These results for (001) QW's are also valid for (111) QW's, since all expressions here for (001) QW's can be transformed to those for (111) QW's only by substituting γ_2 for γ_3 in Q_k.

2. (110) QW

The zeroth-order perturbed wave functions of the heavy- and light-hole states can be written as

$$|\mathrm{hh}(+)\rangle_{0\mathrm{th}}=\frac{1}{\sqrt{2}}(1+\alpha)^{1/2}|\tfrac{3}{2},\tfrac{3}{2}\rangle -\frac{1}{\sqrt{2}}(1-\alpha)^{1/2}|\tfrac{3}{2},-\tfrac{1}{2}\rangle\ , \tag{A6}$$

$$|\mathrm{lh}(+)\rangle_{0\mathrm{th}}=\frac{1}{\sqrt{2}}(1-\alpha)^{1/2}|\tfrac{3}{2},\tfrac{3}{2}\rangle +\frac{1}{\sqrt{2}}(1+\alpha)^{1/2}|\tfrac{3}{2},-\tfrac{1}{2}\rangle\ , \tag{A7}$$

respectively, where $\alpha=Q_k/(Q_k^2+R_k^2)^{1/2}$. Using these zeroth-order perturbed wave functions, one can derive the optical-matrix elements in the model neglecting the SO bands, as was done in Ref. 22. The derived optical-matrix elements are independent of the well width. It has been shown in Ref. 22 that, for the heavy-hole transition, $|M_x|^2$ and $|M_y|^2$ are slightly larger and smaller than $\frac{2}{3}P^2$, respectively.

The first-order perturbed wave function for the heavy-hole state can be written using the above zeroth-order perturbed wave functions as

$$|\mathrm{hh}(+)\rangle_{1\mathrm{st}}=|\mathrm{hh}(+)\rangle_{0\mathrm{th}}+\frac{(1+\alpha)^{1/2}R_k+(1-\alpha)^{1/2}Q_k}{\Delta}\left[-\frac{(1+\alpha)^{1/2}Q_k-(1-\alpha)^{1/2}R_k}{2Q_k}|\mathrm{lh}(+)\rangle_{0\mathrm{th}}+|\tfrac{1}{2},-\tfrac{1}{2}\rangle\right]\ . \tag{A8}$$

Since α is close to 1 in general, it is clear that the coefficient for $|\mathrm{lh}(+)\rangle_{0\mathrm{th}}$ in Eq. (A8) is negative, while that for $|\frac{1}{2},-\frac{1}{2}\rangle$ is positive. Therefore, it can be deduced from Eqs. (12a) and (12b) that $|M_x|^2$ increases while $|M_y|^2$ decreases for the heavy-hole transition as the well width decreases. Thus the in-plane anisotropy increases with decreasing well width. A similar argument can be obtained for other low-symmetry QW's such as $(11N)$ QW's with $N\neq 0$ or 1. The in-plane anisotropies in such $(11N)$ QW's are expected to become noticeably larger than the predicted values[18] within the four-band model when the well width is narrow.

*Present address: Optoelectronics & Microwave Devices Laboratory, Mitsubishi Electric Corporation, 4-1 Mizuhara, Itami, Hyogo 664, Japan.

[1]S. W. Corzin, R. H. Yan, and L. A. Corldren, in *Quantum Well Lasers,* edited by P. S. Zory, Jr. (Academic, San Diego, 1993), p. 55.

[2]H. Kobayashi, H. Iwamura, T. Saku, and K. Otsuka, Electron. Lett. **19**, 166 (1983).

[3]M. Yamada, S. Ogita, M. Yamagishi, K. Tabata, N. Nakaya, M. Asada, and Y. Suematsu, Appl. Phys. Lett. **45**, 324 (1984).

[4]M. Yamanishi and I. Suemune, Jpn. J. Appl. Phys. **23**, L35 (1984).

[5]G. Bastard, *Wave Mechanics Applied to Semiconductor Heterostructures* (Les Edition de Physique, Paris, 1990), p. 248.

[6]M. F. H. Schuurmans and G. W. 't Hooft, Phys. Rev. B **31**, 8041 (1985).

[7]R. Eppenga, M. F. H. Schuurmans, and S. Colak, Phys. Rev. B **36**, 1554 (1987).

[8]B. Gill, P. Lefebre, P. Boring, K. J. Moore, G. Duggun, and K. Woodbridge, Phys. Rev. B **44**, 1942 (1991).

[9]C. Y. Chao and S. L. Chuang, Phys. Rev. B **46**, 4110 (1992).

[10]G. Hatakoshi, K. Inata, M. Ishikawa, M. Okajima, and Y. Uematsu, IEEE J. Quantum Electron. **27**, 1476 (1991).

[11]J. C. Phillips, *Bonds and Bands in Semiconductors* (Academic, New York, 1973), Chap. 7.

[12]C. T. H. F. Liedenbaum, A. Valster, A. L. G. J. Severens, and G. W. 't Hooft, Appl. Phys. Lett. **57**, 2698 (1990).

[13]R. P. Schneider, Jr., R. P. Bryan, E. D. Jones, and J. A. Lott, Appl. Phys. Lett. **63**, 1240 (1993).

[14]M. D. Dawson and G. Duggan, Phys. Rev. B **47**, 12 598 (1993).

[15]S. Kamiyama, T. Uenoyama, M. Mannoh, and K. Ohnaka, in *Extended Abstract of International Conference on Solid State Devices and Materials* (Yokohama, Japan, 1994), p. 250.

[16]Y. Kajikawa, M. Hata, T. Isu, and Y. Katayama, Surf. Sci. **267**, 501 (1992).

[17]D. Gershoni, I. Brener, G. A. Baraff, S. N. Chu, L. N. Pfeiffer, and K. West, in *GaAs and Related Compounds,* edited by G. Stringfellow, IOP Conf. Ser. No. 120 (Institute of Physics and Physical Society, Bristol, UK, 1992), p. 419.

[18]Y. Kajikawa, O. Brandt, K. Kanamoto, and N. Tsukada, in *Workbook of Eighth International Conference on Molecular Beam Epitaxy* (Osaka, Japan, 1994), p. 371.

[19]H. Kamada, K. Oe, R. Bhat, M. Koza, and T. Ikegami, in *GaAs and Related Compounds,* edited by F. Hasegawa and Y. Takeda, IOP Conf. Ser. No. 129 (Institute of Physics and Physical Society, Bristol, UK, 1993), p. 247.

[20]D. Sun, E. Towe, M. J. Hayduck, and R. Boneck, Appl. Phys. Lett. **63**, 2881 (1993).

[21]D. Sun, R. H. Henderson, and E. Towe, in *Extended Abstract of International Conference on Solid State Devices and Materials* (Ref. 15), p. 229.

[22]Y. Kajikawa, M. Hata, and T. Isu, Jpn. J. Appl. Phys. **30**, 1944 (1991). Workbook of Eighth International Conference on Molecular Beam Epitaxy (Osaka, Japan, 1994), p. 271.

[23]D. Vakhshoori, Appl. Phys. Lett. **65**, 259 (1994).

[24]T. Ohtoshi, T. Kuroda, A. Niwa, and S. Tsuji, Appl. Phys. Lett. **65**, 1886 (1994).

[25]S. Nojima, Phys. Rev. B **47**, 13 535 (1993).

[26]J. M. Luttinger and W. Kohn, Phys. Rev. **97**, 869 (1955).

[27]D. S. Citrin and Y. C. Chang, Phys. Rev. B **40**, 5507 (1989).

[28]Y. Kajikawa, Phys. Rev. B **47**, 3649 (1993).

[29]Y. Kajikawa, Ph.D. thesis, University of Tokyo, 1994.

[30]P. Lawaetz, Phys. Rev. B **4**, 3460 (1971).

[31]M. P. C. M. Krijn, Semicond. Sci. Technol. **6**, 27 (1991).

[32]S. O'Brien, D. P. Bour, and J. R. Shealy, Appl. Phys. Lett. **53**, 1859 (1988).

[33]H. Tanaka, Y. Kawamura, S. Nojima, K. Wakita, and H. Asahi, Appl. Phys. Lett. **61**, 1713 (1987).

[34]K. Hirakawa, Y. Hashimoto, and T. Ikoma, Appl. Phys. Lett. **57**, 2555 (1990).

[35]G. J. Sonek, J. M. Ballentyne, Y. J. Chen, G. M. Carter, S. W. Brown, E. S. Kotels, and J. P. Salerno, IEEE J. Quantum Electron. **QE-22**, 1015 (1986).

[36]Y. Kajikawa, N. Sugiyama, T. Kamijoh, and Y. Katayama, Jpn. J. Appl. Phys. **28**, L1022 (1989).